Polymer Journal (2019) 51:739–751
https://doi.org/10.1038/s41428-019-0193-4

FOCUS REVIEW

Primary to quaternary structures of molecular assemblies

Shunsaku Kimura[1]

Received: 22 February 2019 / Revised: 22 March 2019 / Accepted: 22 March 2019 / Published online: 25 April 2019

Abstract

Several kinds of molecular assemblies are prepared from polypeptides and cyclic peptides at various levels of structural regularities, which lead to the current proposal to categorize molecular assemblies into primary to quaternary structures. The categorization places a focal point on phase separation in molecular assemblies because highly sophisticated molecular assemblies have hierarchical organizations of molecules that accompany phase separation and the regular arrangement of chromophores, as frequently observed in nature. Examples of the peptide-based molecular assemblies are thus explained in accordance with the primary to quaternary structures with the aim of implementing nanomaterials in the coming era.

Introduction

Molecular assemblies in aqueous environments are ubiquitous in the biological world and have been extensively studied on the basis of different building blocks of lipids [1, 2], proteins [3–5], nucleic acids [6], saccharides [7], and synthetic molecules [8]. The shape control of molecular assemblies is one of the major subjects pursued in this field, and the morphologies (especially of copolymer assemblies) are now well understood in terms of the volumetric ratios of their different blocks of amphiphilic block polymers [9] as well as the packing parameter derived from the cross-sectional area of the hydrophilic core and the length of the hydrophobic chain [10]. With increasing reports on molecular assemblies, the categorization of molecular assemblies is proposed, for example, according to assembly mechanisms [8] and structural features [11]. The former categorization includes four kinds of mechanisms: (1) polymerization-induced self-assembly [12], (2) control by interactions with the surrounding medium [13], (3) crystallization-driven self-assembly [14], and (4) multicompartment systems. The latter categorization relies on hierarchical self-assemblies, where clusters are starting units as the primary structure that grow into nanocapsules as the secondary structure and finally into 2D or 3D self-assemblies as the tertiary structure. In contrast to these perspectives, a new categorization for primary to quaternary structures of molecular assemblies are presented in this review based on the phase separation or nonrandom distribution of components in molecular assemblies, which is intended to provide a foundation to construct sophisticated complex molecular assemblies that appear in nature. For example, the raft model describes phase separation in cell membranes due to the clustering of specific components, which is a general observation and closely related to biological functions such as endocytosis and exocytosis [15, 16]. In these cases, shape changes from planar to vesicular membranes originate partly from phase separation of the membrane components.

The primary to quaternary structures of molecular assemblies proposed here are schematically drawn in Fig. 1. The primary structure of molecular assemblies defines the shape of molecular assemblies by a single morphology under dimensional control. Morphologies may be round micelles, cylindrical micelles, planar sheets, curved sheets (including rolled sheets), tubes, polyhedral structures, or vesicles, which are prepared under dimensional control (Fig. 1a). The secondary structure depicts the shapes of molecular assemblies through a combination of primary structures. For example, a combination of tubes and vesicles may generate a round-bottom flask shape with a continuous but phase-separated membrane, where one part of the molecular assembly takes a vesicular shape composed of one or a set of components and the other part takes a tubular shape (Fig. 1b). The tertiary structure is the molecular assembly that apparently shows a single morphology but

✉ Shunsaku Kimura
kimura.shunsaku.4w@kyoto-u.ac.jp

[1] Department of Material Chemistry, Graduate School of Engineering, Kyoto University Kyoto-Daigaku-Katsura, Nishikyo-ku, Kyoto 615-8510, Japan

Fig. 1 **a** Primary [18], **b** secondary [30], **c** tertiary [34], and **d** quaternary [47] structures of molecular assemblies in light of phase separation

has characteristic structural features (Fig. 1c). Let us discuss the vesicle shape as an example. From the perspective of the primary structure, the vesicle is defined as a spherical molecular assembly with an inner space separated from the outside. When the vesicle has an outer surface that is different from the inner surface in terms of components, the vesicle is classified as possessing a tertiary structure due to the unsymmetric structural feature. The unsymmetric membrane is a general feature of biological membranes, where the components that face the outside differ from the components that face the inside, irrespective of the symmetric planar sheet shape. In the case of biological membranes, the inside and outside of membranes can be differentiated during the preparation process, which enables the directional insertion of proteins and lipids into membranes, as exemplified by the Golgi apparatus [17]. Without relying on such sequential procedures, molecular assemblies that show a tertiary structure in a thermodynamically stable state are difficult to obtain but are challenging and are a prerequisite for the construction of hierarchical molecular assemblies. Another example of a tertiary structure are molecular assemblies that display a regular distribution of chromophores, which is a characteristic structural feature that is directly relevant to functions. The tertiary structure proposed here is therefore crucial and rationalizes the categorization in light of the development of hierarchical molecular assemblies with quaternary structures. The quaternary structure represents a hierarchical organization of molecular assemblies (Fig. 1d). The term "quaternary structure", for example, can be used to explain assemblies of tubes or vesicles that align in a 3D space based on a defined number of molecular assemblies and/or a defined structural regularity that includes the orientation of tubes or vesicles. Tubes come to possess orientation when they have one open end that is different from the other open end on a chemical basis, which allows for two types of hierarchical associations in a parallel and antiparallel way. Therefore, tube bundles should be described based on their quaternary structure.

Primary structure

Curved sheet

Amphiphilic block polypeptides have a sequence of poly(sarcosine)-*b*-(Leu-Aib)$_n$ (the number average molecular weight of approx. 25mer of poly(sarcosine) and $n = 6$) in which the N and C-terminals are generally protected by glycolic acid and methyl ester to make the polypeptides nonionic, forming curved-sheet-shaped molecular assemblies with approx. 250 nm sides (Fig. 2a) [18]. The hydrophobic block takes an α-helical conformation, which drives the association of polypeptides in water. On the basis of AFM images of the sheet, the membrane thickness supports the interdigitated structure [19], which is also supposed to be stabilized by the antiparallel association of α-helices that have a macrodipole. The interdigitated adjacent helices can associate tightly by tilting slightly with each other to accommodate isobutyl groups of Leu side chains at the interface of two helices in a line (Fig. 3) [20]. The successive tilting of helices is therefore the cause of the formation of the curved sheets.

It is interesting to note that the sizes of the curved sheets are well controlled to be approx. 250 nm in the case when the poly(sarcosine) block is an approx. 25 mer. When the poly(sarcosine) chain length was extended to a 60mer, the sheet size decreased sharply to tiny squares with side lengths of approx. 20 nm [21]. The sheets have four edges that possibly expose hydrophobic faces composed of hydrophobic helices to promote the further association of other helical blocks. The long hydrophilic poly(sarcosine) chains, however, can overhang the hydrophobic face to prevent it from growing into larger assemblies. The hydrophobic edges that are concealed by poly(sarcosine) chains are therefore considered to rest in a dormant state, which controls the growth process of the molecular assemblies via association with new components, resulting in a homogeneous size distribution as a whole (Fig. 4). The size of sheets is thus controllable by adjusting the poly(sarcosine) block length.

Rolled sheet

As described above, the hydrophilic poly(sarcosine) block plays an essential role in the ability of the hydrophobic edges of sheets to grow into larger assemblies. Taking this point into the molecular design, the A_2B-type amphiphilic polypeptides, which have two hydrophilic poly(sarcosine) blocks and one hydrophobic helix, are expected to suppress the growth of molecular assemblies by effectively covering the hydrophobic edge with two hydrophilic blocks and also to inhibit a sticking process of the hydrophobic edges due to steric hindrance. Figure 3 shows two types of hydrophobic

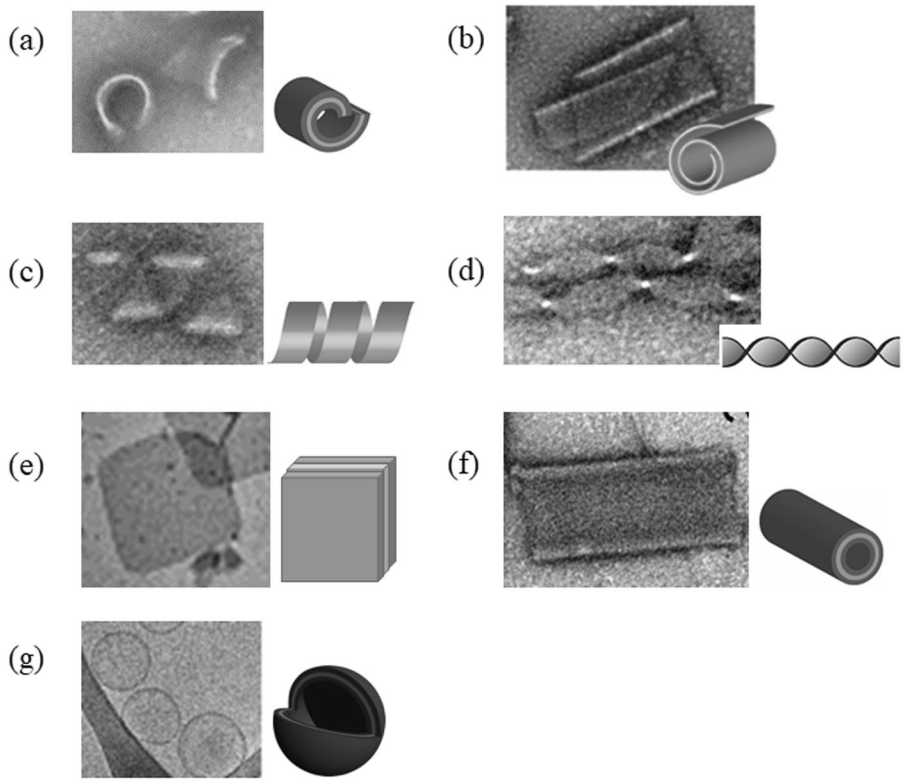

Fig. 2 Primary structures of molecular assemblies. **a** Curved sheet [18], **b** rolled sheet [22], **c** helical ribbon [23], **d** twisted ribbon [23], **e** planar sheet [24], **f** tube [18], and **g** vesicle [24]

edges: front and lateral edges. The curved sheet grows in the lateral and longitudinal directions via association of amphiphilic polypeptides with the front and lateral edges, respectively. With two hydrophilic poly(sarcosine) chains, the curved sheet has difficulty sticking to the front edges, leading to formation of a rolled sheet shape. Indeed, (poly(sarcosine))$_2$-His-(L-Leu-Aib)$_6$ forms molecular assemblies with a rolled-sheet morphology after heat treatment at 90 °C for 1 h (Fig. 2b) [22]. The process requires heat activation of the edges to expose the hydrophobic face by uncovering two poly(sarcosine) chains of (poly(sarcosine))$_2$-His-(L-Leu-Aib)$_6$, where two poly(sarcosine) chains make the polypeptide soluble in water. The layer spacing of the rolled sheets was changeable from approx. 9 to approx. 19 nm as the pH decreased from 7.4 to 5.0 due to electrostatic repulsion caused by histidine protonation.

The A_3B-type amphiphilic polypeptide of (poly(sarcosine))$_3$-His$_2$-(L-Leu-Aib)$_6$ formed molecular assemblies with a helical-ribbon morphology after heat treatment at 70 °C for 6 h at pH 5.0 (Fig. 2c) and with a twisted-ribbon morphology after heat treatment at 70 °C for 6 h at pH 3.0 (Fig. 2d) [23]. With three hydrophilic poly(sarcosine) chains, the curved sheet has difficulty growing longitudinally via association of the amphiphilic polypeptides with the lateral edge, resulting in the formation of a helical-ribbon or twisted-ribbon shape instead of a rolled sheet shape. The existence of different morphologies (helical and twisted ribbons) is ascribable to the two histidine protonations of 2+ at pH 3.0 and 1+ at pH 5.0 in which the helix packing is looser at pH 3.0 than pH 5.0 to induce the morphology transformation.

Planar sheet

Molecular assemblies with planar-sheet morphologies were obtained from a mixture of poly(sarcosine)-*b*-(L-Leu-Aib)$_6$ and poly(sarcosine)-*b*-(D-Leu-Aib)$_6$ upon injection into water (Fig. 2e) [24]. In contrast to the association of homochiral helices with slightly tilted helix axes, the association of heterochiral helices, right- and left-handed helices, follows the parallel alignment of helices and leads to formation of planar sheets (Fig. 5). The isobutyl groups of the Leu side chains at the interface of two heterochiral helices in the interdigitated structure can be accommodated on a straight line upon stacking of one helix on the parallel side of the other. It is noted that the self-assembly of left and right-handed molecular screws is favored in general [25] and that Leu-Aib base peptides belong to this class.

The interpretation that the heterochiral association of the right- and left-handed helices is energetically more stable than the homochiral association is supported by the observation that the planar sheet was shown to be preparable by another method that uses the fusion of heterochiral tubes. According to the following section that explains the formation of

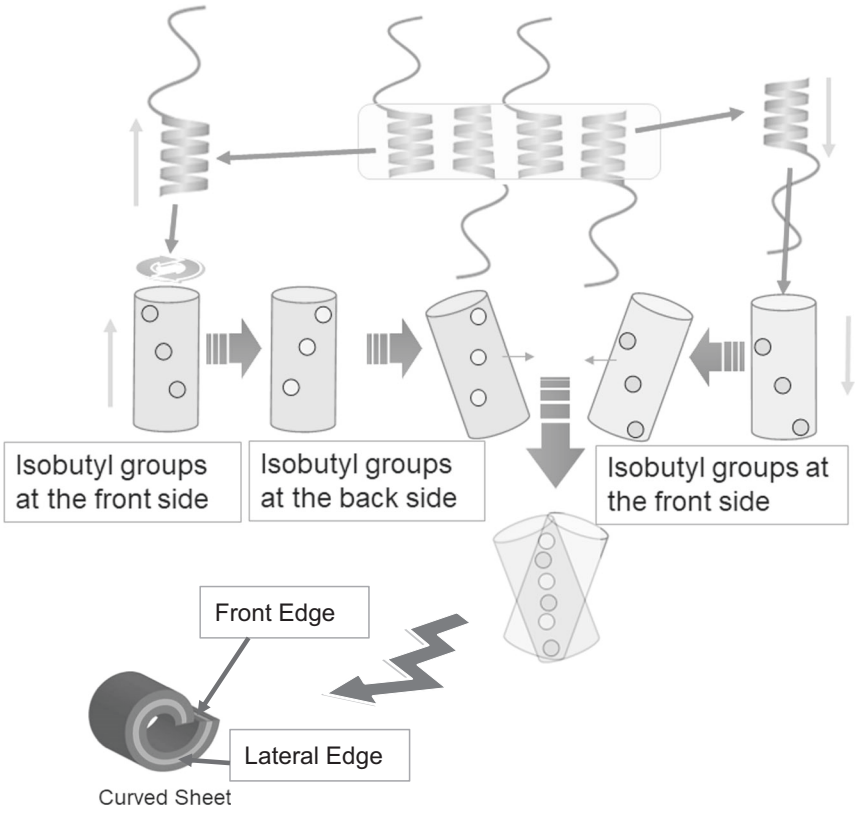

Fig. 3 Schematic illustration of the association mode of two neighboring right-handed helices in the interdigitated monolayer. The rod and circle respectively represent the helix and the isobutyl groups [20]

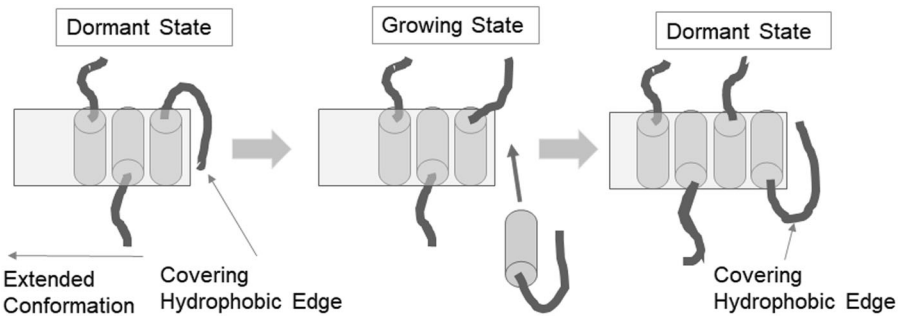

Fig. 4 The hydrophobic edge of molecular assemblies is shielded from water by the overhanging hydrophilic chain to remain in a dormant state. The hydrophilic chain that covers the hydrophobic helix regulates the growth process of the molecular assembly

molecular assemblies with tube morphologies, two kinds of tubes were prepared from poly(sarcosine)-*b*-(L-Leu-Aib)$_6$ and poly(sarcosine)-*b*-(D-Leu-Aib)$_6$ upon heat treatment and were mixed together, followed by heat treatment at 50 °C for 7 h. The tube morphology was converted to a planar sheet morphology via fusion of the two kinds of tubes due to favorable stereocomplex formation between the right- and left-handed helices [24].

Tube (Fig. 1a)

When an ethanol solution of poly(sarcosine)-*b*-(L-Leu-Aib)$_6$ was injected into water, molecular assemblies with curved sheet morphologies were formed. The morphology transformation from curved sheets into tubes occurred after heating at 90 °C for 1 h (Fig. 2f) [18]. Notably, the diameters and lengths of the tubes were approx. 70 nm and 200 nm, respectively, which suggests that the transformation occurs by sticking two opposite sides of the curved sheet together upon heat treatment. The dimensions of the curved sheets were relatively homogeneous, leading to a moderately homogeneous distribution of tube dimensions. Consequently, the tube length was partly elongated to be double upon extension of the heating period to 24 h through the process of sticking two preformed tubes. The present two-step mechanism for molecular assemblies with tube morphologies is in vivid contrast to other tubes via a growing process of a successive association of components [26].

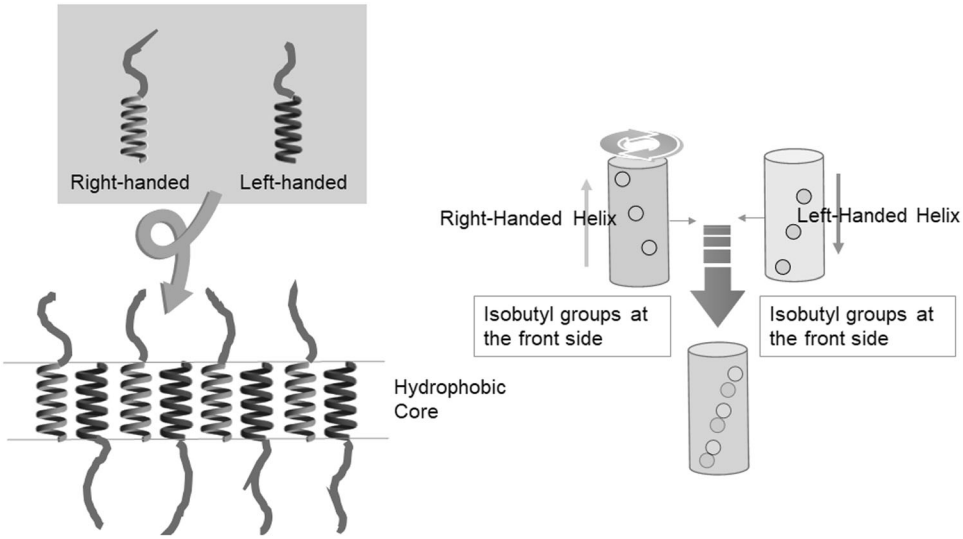

Fig. 5 Schematic illustration of the association mode of two neighboring right and left-handed helices in the interdigitated monolayer. The rod and circle respectively represent the helix and the isobutyl groups

Tube diameters and lengths were found to be changeable by choosing combinations of heterochiral amphiphilic polypeptides with different lengths of hydrophobic blocks [27]. The two-component mixtures of poly(sarcosine)-*b*-(D-Leu-Aib)$_6$ with varying counter parts from poly(sarcosine)-*b*-(L-Leu-Aib)$_7$ to poly(sarcosine)-*b*-(L-Leu-Aib)$_8$ and poly(sarcosine)-*b*-(L-Leu-Aib)$_{10}$ yielded peptide nanotubes of varying dimensions with 200 nm diameters and 400 nm lengths, 70 nm diameters and several micrometer lengths (maximum 30 μm), and 70 nm diameters and 100–600 nm lengths, respectively. These findings support the interpretation that the heterochiral helices favorably associate side-by-side with an interdigitated structure even though the helix lengths differ between the heterochiral helices. The tube formation mechanism is a two-step mechanism for the combination of poly(sarcosine)-*b*-(D-Leu-Aib)$_6$ with poly(sarcosine)-*b*-(L-Leu-Aib)$_7$, which generated intermediate large sheets that result in the formation of tubes with a relatively homogeneous length distribution. On the other hand, the growth mechanism is applicable to combinations of poly(sarcosine)-*b*-(D-Leu-Aib)$_6$ with poly(sarcosine)-*b*-(L-Leu-Aib)$_8$ and poly(sarcosine)-*b*-(L-Leu-Aib)$_{10}$. The small or irregular sheets were formed transiently, which associate at the open ends of tubes and result in a lack of control of the tube lengths.

Vesicle

Vesicles can be prepared from various polypeptides of a combination of poly(sarcosine)-*b*-(D-Leu-Aib)$_6$ and poly(sarcosine)-*b*-(L-Leu-Aib)$_6$ [24], poly(sarcosine)-*b*-(L-Leu-Aib)$_8$ [28], poly(sarcosine)-*b*-(L-Leu-Aib)$_6$-*N*-ethylcarbazole, poly(sarcosine)-*b*-(D-Leu-Aib)$_6$-naphthalimide, and poly(sarcosine)-*b*-(D-Leu-Aib)$_6$-prophyrin [19]. Notably, vesicles prepared from a mixture of poly(sarcosine)-*b*-(L-Leu-Aib)$_6$ and poly(sarcosine)-*b*-(D-Leu-Aib)$_6$ were evaluated to have a weight average diameter of 248 nm and a number average diameter of 228 nm, demonstrating that the PDI was as low as 1.09. The two-step mechanism for vesicle formation is also applicable to cases of a combination of poly(sarcosine)-*b*-(D-Leu-Aib)$_6$ and poly(sarcosine)-*b*-(L-Leu-Aib)$_6$, poly(sarcosine)-*b*-(L-Leu-Aib)$_8$, and poly(sarcosine)-*b*-(L-Leu-Aib)$_6$-*N*-ethylcarbazole, which form membranes with an interdigitated monolayer. The last case showed the intermediate formation of tubes between sheets and vesicles with lengthening of the heating process at 90 °C, which is reasonably explained by the increase in thermodynamic stability in the order of sheets < tubes < vesicles due to the loss of unstable hydrophobic edges in this order. A tube morphology is the most stable shape for poly(sarcosine)-*b*-(L-Leu-Aib)$_6$ to take due to the tight association of helices. A tube morphology followed by a vesicle morphology appeared upon heating in the case of poly(sarcosine)-*b*-(L-Leu-Aib)$_6$-*N*-ethylcarbazole because *N*-ethylcarbazole at the C terminal moderately disturbs the helix association to allow it to take a vesicle morphology. The hydrophobic chromophores of naphthalimide and porphyrin at the C terminals of the hydrophobic helices are too large for amphiphilic polypeptides to take a tube morphology. The large chromophores even changed the membrane structures of poly(sarcosine)-*b*-(D-Leu-Aib)$_6$-naphthalimide and poly(sarcosine)-*b*-(D-Leu-Aib)$_6$-prophyrin to take a bilayer structure on the basis of membrane thickness because these chromophores sterically impair the favorable association property of the helices [19].

The two-step mechanism inspired a new preparative method in which the dimensions of the molecular assembly are controlled by the initial molecular assemblies. This idea was examined via preparation of small vesicles for which

the diameters were determined by the starting molecular assembly of a tube with a 50 nm diameter. A tube with an approx. 50 nm diameter was prepared from a mixture of poly(sarcosine)-*b*-(L-Leu-Aib)$_8$ and poly(sarcosine)-*b*-(D-Leu-Aib)$_7$, followed by the mixing of a nanosheet composed of poly(sarcosine)-*b*-(D-Leu-Aib)$_8$. With heat treatment at 90 °C, vesicles of approx. 60 nm diameter were generated via the fusion of nanosheets to open ends of tubes, followed by transformation into vesicles at the open end [29]. Vesicles were also attainable from a mixture of poly(sarcosine)-*b*-(L-Leu-Aib)$_8$, poly(sarcosine)-*b*-(D-Leu-Aib)$_7$, and poly(sarcosine)-*b*-(D-Leu-Aib)$_8$, but with diameters ranging from approx. 130 nm to approx. 200 nm depending on the composition. Therefore, the tubes acted as a structural template that regulated the sizes of vesicles near the tube diameter upon the membrane fission process.

Secondary structure

Round-bottom-flask-type chimeric morphology (Fig. 1b)

An AB-type chimeric morphology of a vesicle (A) and a tube (B) belongs to the secondary structure. Tubes and vesicles were respectively prepared from poly(sarcosine)-*b*-(L-Leu-Aib)$_6$ and an equimolar mixture of poly(sarcosine)-*b*-(L-Leu-Aib)$_6$ and poly(sarcosine)-*b*-(D-Leu-Aib)$_6$. Interestingly, a mixture of poly(sarcosine)-*b*-(L-Leu-Aib)$_6$ and poly(sarcosine)-*b*-(D-Leu-Aib)$_6$ at a molar ratio of 2:8 or 8:2 provided molecular assemblies with a chimeric morphology of tubes and vesicles, which is called a round-bottom-flask-type morphology (Fig. 6a) [30]. A mixture of preformed tubes and vesicles retained original morphologies upon heat treatment and failed to generate the chimeric morphology. It is therefore considered that the two-step mechanism is also crucial for preparation of molecular assemblies with a chimeric morphology. Indeed, TEM observations revealed that a mixture of poly(sarcosine)-*b*-(L-Leu-Aib)$_6$ and poly(sarcosine)-*b*-(D-Leu-Aib)$_6$ at a molar ratio of 2:8 or 8:2 self-assembled into large planar sheets, which were transformed into a round-bottom-flask-type morphology upon heat treatment. The component amphiphilic polypeptides are allowed to diffuse in the large sheets over 90 °C to induce phase separation in the large sheets with one region of poly(sarcosine)-*b*-(L-Leu-Aib)$_6$ and poly(sarcosine)-*b*-(D-Leu-Aib)$_6$ in a stereocomplex state and the other region including the remainder of the component. With further heat treatment, the former region was forced to take a vesicular morphology, and the latter region was forced to take a tube morphology. As a result, a round-bottom-flask-type morphology surrounded by one continuous membrane was formed.

Test-tube-type chimeric morphology

Another AB-type chimeric morphology is the test-tube-type morphology. Tubes composed of poly(sarcosine)-*b*-(L-Leu-Aib)$_6$ and planar sheets composed of poly(sarcosine)-*b*-(L-Leu-Aib)$_8$ were mixed and heated at 90 °C for 1 h to

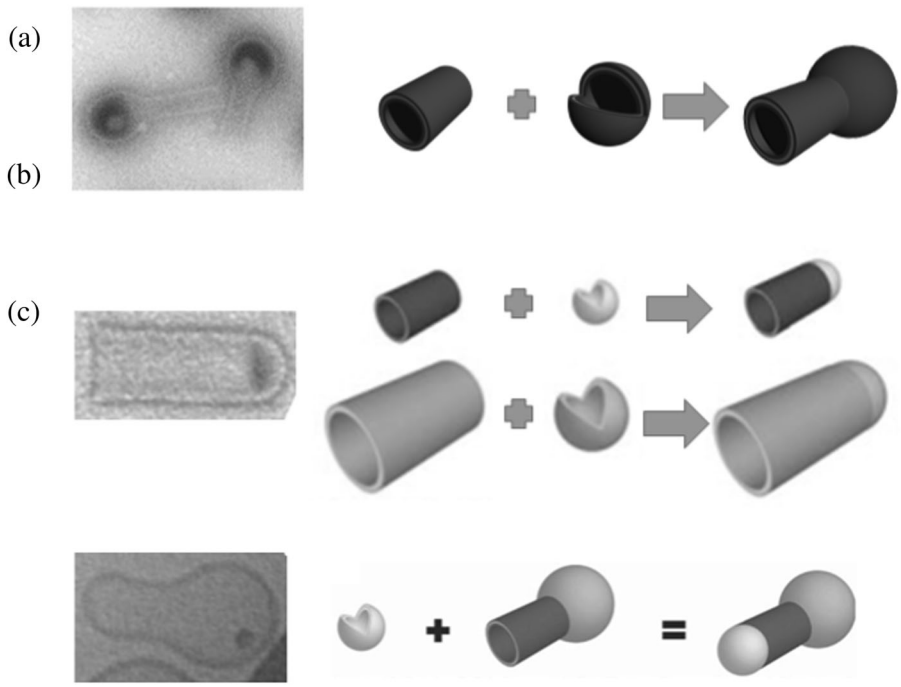

Fig. 6 Secondary structures of molecular assemblies with a round-bottom-flask-type morphology (**a**) [30], a test-tube-type morphology with two different sizes (**b**) [31], and an electric-bulb-type morphology [31]

generate molecular assemblies with a test-tube-type morphology (Fig. 6) [31]. In this case, poly(sarcosine)-*b*-(L-Leu-Aib)$_6$ self-assembled into a tube morphology with an approx. 70 nm diameter and poly(sarcosine)-*b*-(L-Leu-Aib)$_8$ self-assembled into a vesicular morphology with an approx. 70 nm diameter, which joined together to generate a test-tube-type morphology. The test-tube-type morphology was able to be developed into a capsule-type morphology of an ABA-type chimeric morphology upon increasing the amount of planar sheets during incubation, where both open ends of tubes were sealed by vesicular membranes [31].

The larger test-tube-type morphology was obtained by a combination of tubes composed of a mixture of poly(sarcosine)-*b*-(L-Leu-Aib)$_7$ and poly(sarcosine)-*b*-(D-Leu-Aib)$_6$ and planar sheets composed of poly(sarcosine)-*b*-(L-Leu-Aib)$_6$ and poly(sarcosine)-*b*-(D-Leu-Aib)$_6$ (Fig. 6b) [31]. The former tubes have approx. 200 nm diameters, and the latter sheets generate vesicles of approx. 200 nm diameters. The planar sheet sticks to the open end of the tube, followed by a morphology transformation into a vesicular shape. Therefore, the preparation method according to the two-step mechanism is also effective at generating molecular assemblies of test-tube-type morphologies.

Light-bulb-type chimeric morphology

An ABA'-type chimeric morphology was attained by sealing the open end of a round-bottom-flask-type morphology (Fig. 6c) [31]. Round-bottom flask assemblies were prepared from a mixture of poly(sarcosine)-*b*-(L-Leu-Aib)$_6$ and poly(sarcosine)-*b*-(D-Leu-Aib)$_6$ at a molar ratio of 2:8 and were mixed with planar sheets composed of poly(sarcosine)-*b*-(L-Leu-Aib)$_8$. Therefore, one open end of a tube with an approx. 70 nm diameter was sealed with a part of a vesicle membrane approx. 200 nm in diameter, and the other open end was sealed with a part of a vesicle membrane approx. 70 nm in diameter, to generate a light-bulb-type chimeric morphology.

Tertiary structure

Unsymmetric vesicle

An equimolar mixture of poly(sarcosine)-*b*-(L-Leu-Aib)$_6$ and poly(sarcosine)-*b*-(D-Leu-Aib)$_6$ afforded vesicles, as described previously. The interdigitated monolayer membrane composed of the heterochiral components indicates that one chiral component extends the hydrophilic block outward and the other chiral component extends it inward. The unsymmetric vesicular membranes are therefore expected to be generated with the help of two kinds of hydrophilic blocks of different sizes. The bulkier hydrophilic blocks should be exposed to the outer surface to relieve steric hindrance. Indeed, unsymmetrical vesicular membranes were successfully prepared from a binary heterochiral mixture of the A_3B-type ((poly(sarcosine))$_3$-*b*-(L-Leu-Aib)$_6$) and AB-type (poly(sarcosine)-*b*-(D-Leu-Aib)$_6$) polypeptides (Fig. 7) [32]. When guest polypeptides of the AB-type that had a disulfide group at the terminus of the hydrophilic block were accommodated in the unsymmetric vesicle, the disulfide group of (lipoic acid)-poly(sarcosine)-*b*-(L-Leu-Aib)$_6$ became located at the outside of the vesicle, while that of (lipoic acid)-poly(sarcosine)-*b*-(D-Leu-Aib)$_6$ became located inside of the vesicle in accordance with the chirality of the guest polypeptide. The formation of the unsymmetric membrane was confirmed by the selective adsorption of gold nanoparticles on the surfaces. The chirality of the helix block of the guest polypeptides therefore determines the outward or inward orientation of the guest polypeptides in the unsymmetric membrane.

The unsymmetric vesicles were applied for near-infrared fluorescence imaging of tumor tissues [33]. Indocyanine green (ICG) was connected to the N terminal of poly(sarcosine)-*b*-(L- or D-Leu-Aib)$_6$. When ICG-poly(sarcosine)-*b*-(L-Leu-Aib)$_6$ was incorporated into the unsymmetric vesicle composed of (poly(sarcosine))$_3$-*b*-(L-Leu-Aib)$_6$ and poly(sarcosine)-*b*-(D-Leu-Aib)$_6$, ICG was exposed to the outside. On the other hand, ICG of ICG-poly(sarcosine)-*b*-(D-Leu-Aib)$_6$ was concealed in the vesicle. When these vesicles were injected into tumor-bearing mice via the tail vein, the latter vesicle was found to accumulate in the tumor more than the former vesicle. Further, the degree of activation of the immune system was less than the former vesicle. Even though the mixing rate of the ICG-labeled polypeptide was as low as 2 mol%, its concealment inside the vesicle facilitated positive results in tumor imaging.

Phase-separated tube (Fig. 1c)

Two kinds of tubes were prepared from poly(sarcosine)-*b*-(L-Leu-Aib)$_6$ and poly(*N*-ethyl glycine)-*b*-(L-Leu-Aib)$_6$. These two kinds of tubes were shown to stick together after heat treatment at 50 °C for 24 h in the presence of 5% trifluoroethanol. The distribution of poly(sarcosine)-*b*-(L-Leu-Aib)$_6$ in the connected tube was evaluated by staining with Au nanoparticles in the presence of (lipoic acid)-poly(sarcosine)-*b*-(L-Leu-Aib)$_6$, which behaves similarly to poly(sarcosine)-*b*-(L-Leu-Aib)$_6$ in the tube. All components were able to diffuse laterally in tube membranes at 50 °C in the presence of 5% trifluoroethanol. After further incubation at 90 °C for 1 h, however, temperature-induced phase separation was observed in the tubes, which is ascribed to the association of poly(*N*-ethyl glycine) in the tube over the cloud point temperature of approx. 70 °C (Fig. 8) [34]. This

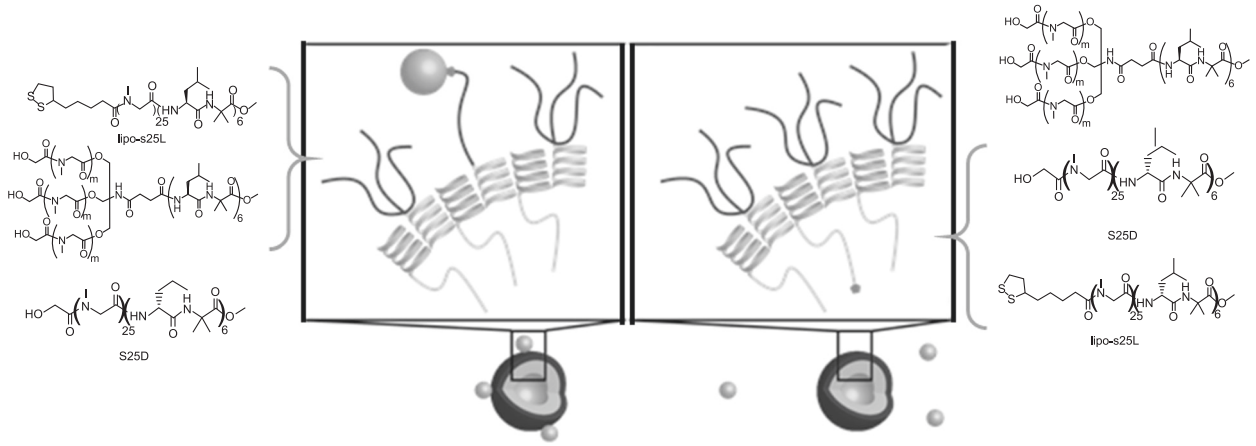

Fig. 7 Tertiary structure of unsymmetric vesicles [32]. Left panel: Lipoic acids extend outward because the chirality of the lipoic acid-polypeptide is the same as the A_3B-type host polypeptide. Right panel: Lipoic acids are concealed inward because the chirality of the lipoic acid-polypeptide is the same as the AB-type host polypeptide. The addition of gold nanoparticles to the unsymmetric vesicles results in labeling the unsymmetric vesicle in the left panel, but no labeling of the vesicle in the right panel occurs

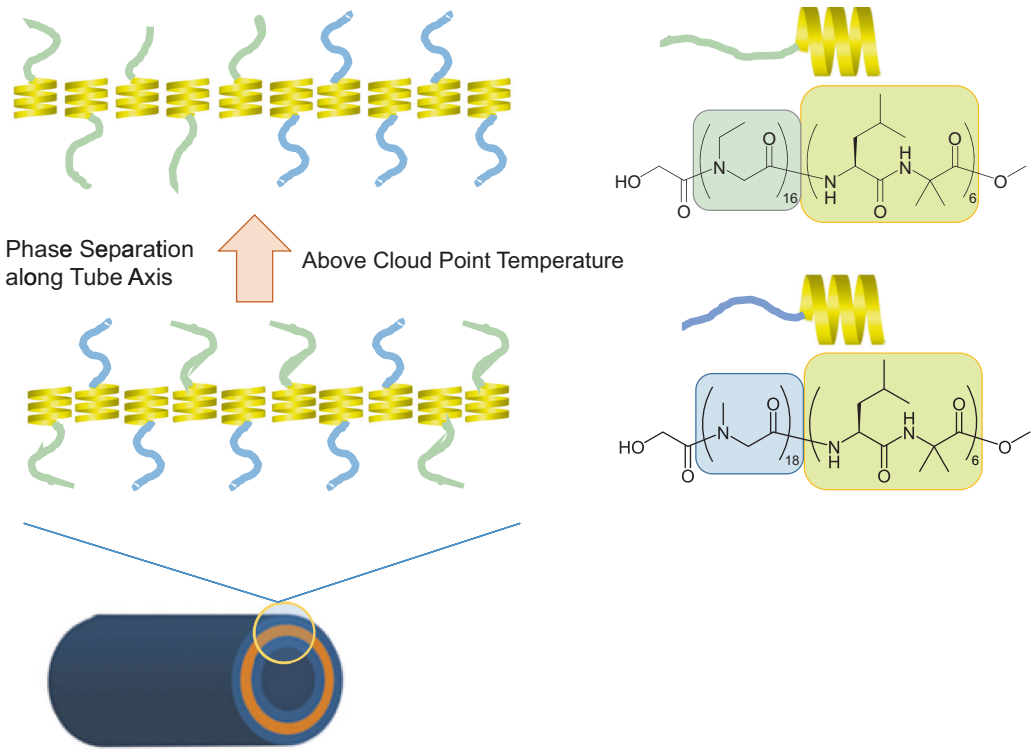

Fig. 8 Tertiary structure of a phase-separated tube [34]. Left panel: Two types of amphiphilic polypeptides, poly(sarcosine)-*b*-(L-Leu-Aib)$_6$ and poly(*N*-ethyl glycine)-*b*-(L-Leu-Aib)$_6$, are miscible in the membrane when the mixture is injected in water. Upon raising the temperature over the cloud point of poly(*N*-ethyl glycine) displayed on molecular assemblies, phase-separation in the membrane is induced in the presence of trifluoroethanol

kind of phase separation in tubes is driven by the thermal response of hydrophilic poly(*N*-ethyl glycine), for which the mechanism is categorized into the hydrophilic-region-driven type.

There was another way to prepare tubes with temperature-induced phase separation. A ternary mixture of poly(sarcosine)-*b*-(L-Leu-Aib)$_6$, poly(*N*-ethyl glycine)-*b*-(L-Leu-Aib)$_6$, and (lipoic acid)-poly(sarcosine)-*b*-(L-Leu-

Aib)$_6$ was incubated at 50 °C for 24 h in the presence of 5% trifluoroethanol, followed by further incubation at 90 °C for 1 h (Fig. 8). A Au nanoparticle adsorption assay revealed that the ratio of the phase-separated tubes amounted to 40% of the total tubes. Notably, the addition of trifluoroethanol was a prerequisite for phase separation, which is necessary for the components to diffuse laterally in membranes due to loosening of the helix packing in the presence of a good solvent, such as trifluoroethanol.

The possibility of obtaining phase-separated tubes just by joining two kinds of tubes was explored [35]. Two kinds of tubes were prepared from a mixture of poly(sarcosine)-*b*-(L-Leu-Aib)$_6$ and poly(sarcosine)-*b*-(L-Leu-Aib)$_6$-ethylcarbazole (9/1 mol/mol) and a mixture of poly(sarcosine)-*b*-(D-Leu-Aib)$_6$ and poly(sarcosine)-*b*-(D-Leu-Aib)$_6$-naphthalimide (9/1 mol/mol), and were mixed together at 15 °C. The phase separation can be evaluated by measuring the average distance between two kinds of fluorophores using the Förster resonance energy transfer method. There was a fraction of extended tubes but no mixing of the chromophores. The stereocomplex formation between the right- and left-handed helices at the open ends of tubes is the driving force to join two kinds of tubes, but the temperature should be kept as low as 15 °C to suppress mixing of the components in the joined membranes.

An attempt to join the two kinds of tubes was made using a type of sticking agent [36]. Tubes were prepared from adenine-poly(sarcosine)-*b*-(L-Leu-Aib)$_6$ and were chelated with Cu(II) ions. The Cu(II)-chelated tubes were mixed with Cu(II)-free tubes, which were incubated at 50 °C. TEM images revealed the existence of phase-separated tubes showing Cu(II)-chelated and Cu(II)-free regions, but with time, the entire tube region was chelated with Cu(II) ions. The phase-separated tubes transiently appeared, probably because Cu(II) ions could be transferred from one site of adenine moieties to a neighboring site with the help of dynamic movements of poly (sarcosine) chains to ultimately be distributed on the entire tube.

Cyclic peptide nanotubes with a regular chromophore alignment

Apart from molecular assemblies in water, where hydrophobic interaction is the driving force to associate molecules, hydrogen bonds can effectively operate to associate molecules in a directional way due to the structural limitation of the location of the H-atom that is nearly on a line between two groups of hydrogen donors and acceptors. Using hydrogen bonds to associate molecules therefore enables the preparation of molecular assemblies of tubes [26, 37–39] and capsules [40]. Tubes prepared from cyclic peptides upon stacking on top of one other have been attracting much attention and are named cyclic peptide nanotubes (cPNTs). With respect to external functionalization of cPNTs by aligning chromophores in-line along PNT surfaces, various molecular designs incorporating salt bridges [41, 42] and a long alkyl chain with diacetylene [43] into component side chains are reported. These cPNTs show regular alignments of side chains along cPNT surfaces, which are categorized into molecular assemblies of tertiary structures. cPNTs with tertiary structures can also be prepared based on the sequence of cyclic peptides. A combination of α-amino acids and β-amino acids is one way to align the side chains of α-amino acids in-line on cPNT surfaces (Fig. 9a) [44]. A cyclic hexapeptide composed of L and D-α-amino acids and four β-alanines was designed to self-assemble into cPNTs by stacking on top of each other under the constraint of maximizing the number of intermolecular hydrogen bonds between cyclic peptides. Upon cPNT formation, the respective side chains of L and D-α-amino acids came to be aligned in-line along the cPNT surface. Another way to construct cPNTs with a tertiary structure is to incorporate a sequence of ethylenediamine-succinic acids into sequences composed of β-amino acids (Fig. 9b) [45, 46]. The chromophore attached at the side chain of the β-amino acid component becomes located at a position slightly deviated from the top of the other cyclic peptide. Consequently, the chromophores are aligned in a helical way along the cPNT surface.

Quaternary structure

Four-cPNT bundle (Fig. 1d)

cPNTs have a strong tendency to associate into bundles, where the association numbers of cPNTs are generally out of regulation to afford cPNT bundles of various thicknesses. When cPNT bundles have a defined association number, the bundles come to possess a higher regularity in the structure, which is rationally designated as the quaternary structure. A hydrophilic cyclic tetra-β-peptide with guanine at the side chain was found to construct a four-peptide-nanotube bundle with the formation of a guanine quadruplex (G-quartet) (Fig. 10a) [47]. In the presence of K^+ ions, the quadruplication of four cyclic peptides occurred to form sheets, which stack due to π-π interactions to grow into the quadruple bundle of cPNTs. TEM observations revealed cPNT bundles with uniform diameters of 7–8 nm.

cPNT bundle in a parallel dipole orientation

cPNTs prepared from cyclic β-peptides possess a macrodipole moment along the long axis due to the perpendicular

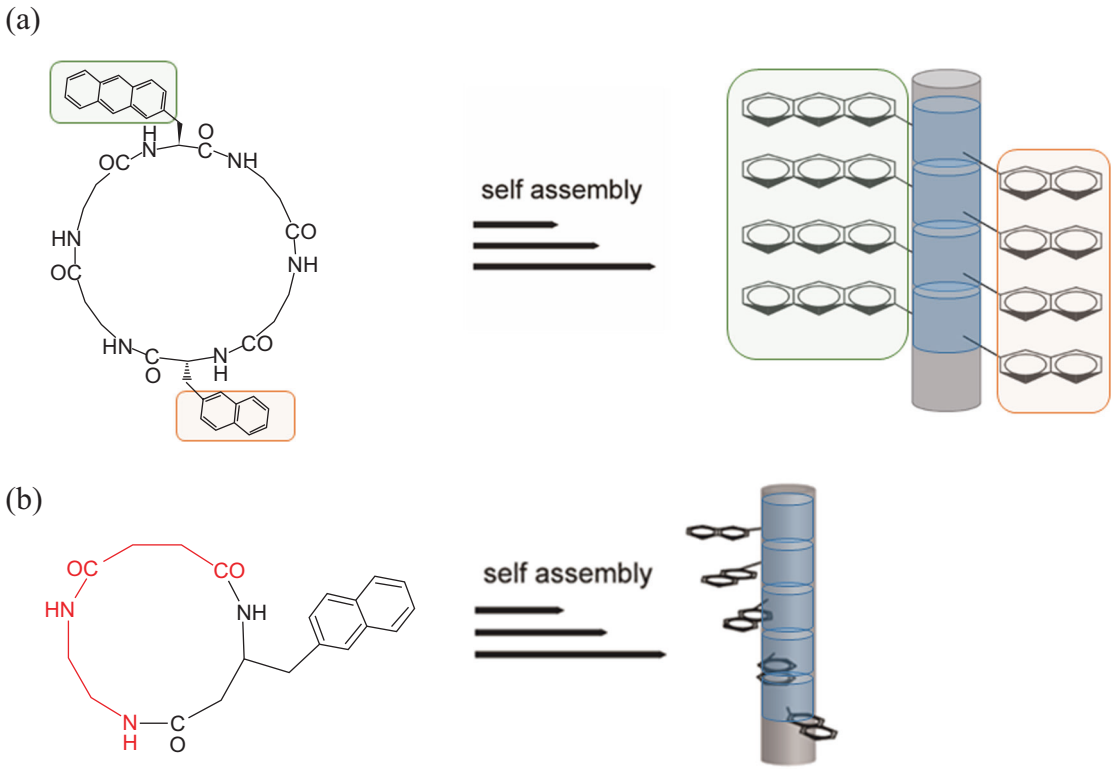

Fig. 9 Tertiary structures of nanotubes with surfaces that have regular chromophore alignments. **a** A sequence of L-α-amino acid, D-α-amino acid, and four β-alanines [44]. **b** A sequence of β-naththylalanine and ethylenediamine-succinic acid [45]

and directional orientation of amide bonds against the planar cyclic skeleton. cPNTs therefore take an antiparallel dipole orientation in cPNT bundles. The addition of bis-cyclic β-peptides to the cPNT formation process promotes a parallel-dipole orientation in the cPNT bundles by stapling adjacent cPNTs (Fig. 10b) [48]. As a consequence of the remaining macrodipole, the cPNT bundles became susceptible to the electric field to induce deformation, reflecting an increase in the piezoelectric coefficient by stapling.

Dynamic transformation of secondary structures

Vesicle fusion

The dynamics of molecular assemblies can reveal details of the structural features of molecular assemblies. As described before, a mixture of poly(sarcosine)-*b*-(L-Leu-Aib)$_6$ and poly(sarcosine)-*b*-(D-Leu-Aib)$_6$ self-assembled into vesicles after heating at 90 °C. This temperature is critical for vesicle formation and is found to be the phase-transition temperature of the vesicle membrane. Vesicles fused together, which was followed by fission back to their original sizes above 90 °C [28]. The membrane fluidity is thus a prerequisite but not enough for vesicle fusion because poly(sarcosine)-*b*-(L-Leu-Aib)$_8$ vesicles possessed fluidic membranes but failed to fuse with each other. The high bending energy stored in poly(sarcosine)-*b*-(L-Leu-Aib)$_6$ and poly(sarcosine)-*b*-(D-Leu-Aib)$_6$ vesicular membranes is considered to be another factor for vesicle fusion. In the case of vesicles composed of a mixture of poly(sarcosine)-*b*-(L-Leu-Aib)$_6$ and poly(sarcosine)-*b*-(D-Leu-Aib)$_6$, the vesicles can exchange components with the same kind of vesicles and even with other polypeptide vesicles via fusion and fission at 90 °C, even though there is no exchange at lower temperatures.

Partial disruption from secondary to primary structure

The round-bottom-flask morphology of the secondary structure was downgraded to a tube or vesicle morphology of the primary structure, where the tubular or vesicular region was selectively disrupted by a pH change [49]. Three types of round-bottom-flask-shaped molecular assemblies were prepared from the combinations of (**1**) tubes of (poly(sarcosine))$_3$-(L-His)$_2$-(L-Leu-Aib)$_6$ and planar sheets of a mixture of poly(sarcosine)-*b*-(L-Leu-Aib)$_6$ and poly(sarcosine)-*b*-(D-Leu-Aib)$_6$, (**2**) tubes of poly(sarcosine)-*b*-(D-Leu-Aib)$_6$ and planar sheets

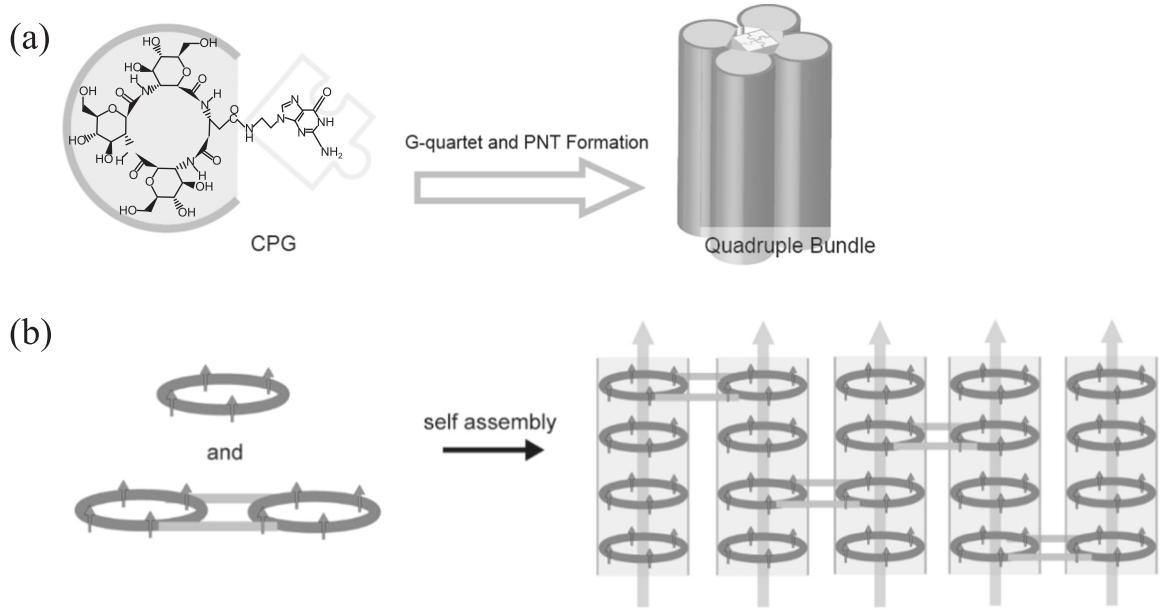

Fig. 10 Quaternary structures of molecular assemblies. **a** Quadruple bundle of cPNTs using a guanine-quartet motif [47]. **b** cPNT bundle in a parallel dipole orientation obtained by stapling cPNTs with bis-cyclic peptides [48]

of a mixture of (poly(sarcosine))$_3$-(L-His)$_2$-(L-Leu-Aib)$_6$ and poly(sarcosine)-*b*-(D-Leu-Aib)$_6$, and (**3**) tubes of poly(sarcosine)-*b*-(L-Leu-Aib)$_6$ and planar sheets of a mixture of (poly(sarcosine))$_3$-(L-His)$_2$-(L-Leu-Aib)$_6$ and poly(sarcosine)-*b*-(D-Leu-Aib)$_6$, all of which formed the secondary structure of the round-bottom-flask shape morphology upon heat treatment at 90 °C in pH 7.4 buffer [49]. The relations of the morphologies with the components are simple to describe in that tubes are formed from homochiral amphiphilic polypeptides and planar sheets from the combinations of heterochiral amphiphilic polypeptides. When tubes and planar sheets are mixed and heated at 90 °C, two types of primary structures join together, followed by transformation from the planar-sheet moiety to the vesicular moiety, leading to the round-bottom-flask shape morphology in accordance with the two-step mechanism. One component of (poly(sarcosine))$_3$-(L-His)$_2$-(L-Leu-Aib)$_6$ is used here to determine its distribution in the secondary structure because molecular assemblies of tubes and vesicles containing (poly(sarcosine))$_3$-(L-His)$_2$-(L-Leu-Aib)$_6$ are disrupted upon heat treatment at 70 °C at pH 5.0 due to protonation of the His dipeptide moiety. It is therefore indicated that the distribution of (poly(sarcosine))$_3$-(L-His)$_2$-(L-Leu-Aib)$_6$ in either the tube region or the vesicular region in the round-bottom-flask shape morphology is assignable whether the remaining molecular assemblies after heat treatment at 70 °C at pH 5.0 are vesicles or tubes. The round-bottom-flask molecular assemblies were found to leave behind vesicles for (**1**), tubes for (**2**), and vesicles for (**3**). Originally, (poly(sarcosine))$_3$-(L-His)$_2$-(L-Leu-Aib)$_6$ was present in the tubular region for (**1**), in the vesicular region for (**2**), and in the vesicular region for (**3**). In the last case, (poly(sarcosine))$_3$-(L-His)$_2$-(L-Leu-Aib)$_6$ therefore diffused from the vesicular region to the tubular region upon heat treatment at 70 °C, rearranging the components in the round-bottom-flask morphology in the presence of (poly(sarcosine))$_3$-(L-His)$_2$-(L-Leu-Aib)$_6$ in the tubular region and a mixture of poly(sarcosine)-*b*-(L-Leu-Aib)$_6$ and poly(sarcosine)-*b*-(D-Leu-Aib)$_6$ in the vesicular region. Taken together, the membrane stability is estimated to decrease in the order of poly(sarcosine)-*b*-(L-Leu-Aib)$_6$ and poly(sarcosine)-*b*-(D-Leu-Aib)$_6$ > (poly(sarcosine))$_3$-(L-His)$_2$-(L-Leu-Aib)$_6$ and poly(sarcosine)-*b*-(D-Leu-Aib)$_6$ > poly(sarcosine)-*b*-(L-Leu-Aib)$_6$ > (poly(sarcosine))$_3$-(L-His)$_2$-(L-Leu-Aib)$_6$.

Perspectives

Primary to quaternary structures of molecular assemblies are explained herein by citing the reported molecular assemblies. Several specific molecular assemblies remain to be reported from the author's group after improvement of yields. In other words, the reported molecular assemblies were obtained with good yields. Peptides are therefore excellent compounds from which to prepare molecular assemblies at various levels, from primary to quaternary structures. Currently, objective-oriented molecular assemblies have been studied in the biomaterial and nanomaterial fields. For example, nanocarriers that can evade the immune system have been successfully realized [21, 50]. Nanomaterials showing piezoelectricity have also been demonstrated [44]. Specifically, in the latter field, the quaternary structure of nanomaterials is crucial for eliciting the requested performance. It is unique for peptides that the

dense amide bonds can be arrayed regularly, for example, either in parallel or antiparallel, with the use of cyclic peptide nanotubes composed of β or α-amino acids, which is in vivid contrast to polymethacrylamide or other commodity polymers that are extremely difficult to use to achieve ordered structures. Further, chromophores attached to cyclic peptide nanotubes can be aligned regularly in 3D space, where structure is generally limited by chromophores showing crystalline or liquid-crystalline (mesogenic) properties. It is therefore expected that molecular assemblies composed of peptides have high potential in applications for piezoelectric, pyroelectric, conductive, semiconductive, and capacitive nanomaterials.

One interesting facet of peptide nanomaterials appears when they are in contact with a metal substrate. For example, cyclic peptide nanotubes prepared on a gold substrate may change the structure by influencing the mirror image dipole generated in gold [46]. The image dipole effect extends over a few tens of nm from the gold surface. Nanomaterials of molecular assemblies under structural control from primary to quaternary structures will thus provide new physical aspects in nanodimensions, which are promising for widening the scope of nanomaterials.

Acknowledgements This research was partially supported by JSPS KAKENHI Grant Numbers JP16H02279 and JP18K19000.

Compliance with ethical standards

Conflict of interest The authors declare that they have no conflict of interest.

References

1. Kulkarni CV. Lipid self-assemblies and nanostructured emulsions for cosmetic formulations. Cosmetics. 2016;3:37.
2. Angelova MI, Bitbol AF, Seigneuret M, Staneva G, Kodama A, Sakuma Y, Kawakatsu T, Imai M, Puff N. pH sensing by lipids in membranes: the fundamentals of pH-driven migration, polarization and deformations of lipid bilayer assemblies. Bba-Biomembr. 2018;1860:2042–2063.
3. Andersson J, Koper I, Knoll W. Tethered membrane architectures-design and applications. Front Mater. 2018;5:56.
4. Nguyen TK, Ueno T. Engineering of protein assemblies within cells. Curr Opin Struc Biol. 2018;51:1–8.
5. Luo Q, Hou CX, Bai YS, Wang RB, Liu JQ. Protein assembly: versatile approaches to construct highly ordered nanostructures. Chem Rev. 2016;116:13571–632.
6. Lazcano A. Prebiotic evolution and self-assembly of nucleic acids. Acs Nano. 2018;12:9643–7.
7. Tsuchido Y, Fujiwara S, Hashimoto T, Hayashita T. Development of supramolecular saccharide sensors based on cyclodextrin complexes and self-assembling systems. Chem Pharm Bull. 2017;65:318–25.
8. Chen C, Wylie RAL, Klinger D, Connal LA. Shape control of soft nanoparticles and their assemblies. Chem Mater. 2017;29:1918–45.
9. Discher DE, Ahmed F. Polymersomes. Annu Rev Biomed Eng. 2006;8:323–41.
10. Cullis PR, Hope MJ, Tilcock CPS. Lipid polymorphism and the roles of lipids in membranes. Chem Phys Lipids. 1986;40:127–44.
11. Zhang C, Wang F, Patil RS, Barnes CL, Li T, Atwood JL. Hierarchical self-assembly of supramolecular coordination polymers using giant metal-organic nanocapsules as building blocks. Chem-Eur J. 2018;24:14335–40.
12. Warren NJ, Armes SP. Polymerization-induced self-assembly of block copolymer nano-objects via RAFT aqueous dispersion polymerization. J Am Chem Soc. 2014;136:10174–85.
13. Cui HG, Chen ZY, Wooley KL, Pochan DJ. Origins of toroidal micelle formation through charged triblock copolymer self-assembly. Soft Matter. 2009;5:1269–78.
14. Qiu HB, Cambridge G, Winnik MA, Manners I. Multi-armed micelles and block co-micelles via crystallization-driven self-assembly with homopolymer nanocrystals as initiators. J Am Chem Soc. 2013;135:12180–3.
15. Komura S, Andelman D. Physical aspects of heterogeneities in multi-component lipid membranes. Adv Colloid Inter. 2014;208:34–46.
16. Morigaki K, Tanimoto Y. Evolution and development of model membranes for physicochemical and functional studies of the membrane lateral heterogeneity. Bba-Biomembr. 2018;1860:2012–7.
17. Ferguson S, Steyer AM, Mayhew TM, Schwab Y, Lucocq JM. Quantifying Golgi structure using EM: combining volume-SEM and stereology for higher throughput. Histochem Cell Biol. 2017;147:653–69.
18. Kanzaki T, Horikawa Y, Makino A, Sugiyama J, Kimura S. Nanotube and three-way nanotube formation with nonionic amphiphilic block peptides. Macromol Biosci. 2008;8:1026–33.
19. Kim CJ, Kurauchi S, Uebayashi T, Fujisaki A, Kimura S. Morphology change from nanotube to vesicle and monolayer/bilayer alteration by amphiphilic block polypeptides having aromatic groups at C terminal. B Chem Soc Jpn. 2017;90:568–73.
20. Itagaki T, Nobe W, Uji H, Kimura S. Osmotic-shock-resistant vesicle comprising interdigitated monolayer of block polypeptides. Chem Lett. 2018;47:726–8.
21. Hara E, Ueda M, Kim CJ, Makino A, Hara I, Ozeki E, Kimura S. Suppressive immune response of poly-(sarcosine) chains in peptide-nanosheets in contrast to polymeric micelles. J Pept Sci. 2014;20:570–7.
22. Uesaka A, Ueda M, Makino A, Imai T, Sugiyama J, Kimura S. Self-assemblies of triskelion A(2)B-type amphiphilic polypeptide showing pH-responsive morphology transformation. Langmuir. 2012;28:6006–12.
23. Uesaka A, Ueda M, Makino A, Imai T, Sugiyama J, Kimura S. Morphology control between twisted ribbon, helical ribbon, and nanotube self-assemblies with his-containing helical peptides in response to pH change. Langmuir. 2014;30:1022–8.
24. Ueda M, Makino A, Imai T, Sugiyama J, Kimura S. Transformation of peptide nanotubes into a vesicle via fusion driven by stereo-complex formation. Chem Commun. 2011;47:3204–6.
25. Xu F, Khan IJ, McGuinness K, Parmar AS, Silva T, Murthy NS, Nanda V. Self-assembly of left and right-handed molecular screws. J Am Chem Soc. 2013;135:18762–5.
26. Shimizu T. Self-assembly of discrete organic nanotubes. B Chem Soc Jpn. 2018;91:623–68.
27. Ueda M, Makino A, Imai T, Sugiyama J, Kimura S. Rational design of peptide nanotubes for varying diameters and lengths. J Pept Sci. 2011;17:94–99.

28. Ueda M, Makino A, Imai T, Sugiyama J, Kimura S. Temperature-triggered fusion of vesicles composed of right-handed and left-handed amphiphilic helical peptides. Langmuir. 2011;27:4300–4.
29. Watabe N, Kim CJ, Kimura S. Fusion and fission of molecular assemblies of amphiphilic polypeptides generating small vesicles from nanotubes. Biopolymers. 2017;108:e22903.
30. Ueda M, Makino A, Imai T, Sugiyama J, Kimura S. Tubulation on peptide vesicles by phase-separation of a binary mixture of amphiphilic right-handed and left-handed helical peptides. Soft Matter. 2011;7:4143–6.
31. Ueda M, Makino A, Imai T, Sugiyama J, Kimura S. Versatile peptide rafts for conjugate morphologies by self-assembling amphiphilic helical peptides. Polym J. 2013;45:509–15.
32. Uesaka A, Ueda M, Imai T, Sugiyama J, Kimura S. Facile and precise formation of unsymmetric vesicles using the helix dipole, stereocomplex, and steric effects of peptides. Langmuir. 2014;30:4273–9.
33. Uesaka A, Hara I, Imai T, Sugiyama J, Kimura S. Unsymmetric vesicles with a different design on each side for near-infrared fluorescence imaging of tumor tissues. Rsc Adv. 2015;5:14697–703.
34. Hattori T, Itagaki T, Uji H, Kimura S. Temperature-induced phase separation in molecular assembly of nanotubes comprising amphiphilic polypeptoid with poly(*N*-ethyl glycine) in water by a hydrophilic-region-driven-type mechanism. J Phys Chem B. 2018;122:7178–84.
35. Itagaki T, Kurauchi S, Uebayashi T, Uji H, Kimura S. Phase-separated molecular assembly of a nanotube composed of amphiphilic polypeptides having a helical hydrophobic block. ACS Omega. 2018;3:7158–64.
36. Itagaki T, Ueda Y, Itabashi K, Uji H, Kimura S. Joining nanotubes comprising nucleobase-carrying amphiphilic polypeptides. Chimia. 2018;72:842–7.
37. Ghadiri MR, Granja JR, Milligan RA, Mcree DE, Khazanovich N. Self-assembling organic nanotubes based on a cyclic peptide architecture. Nature. 1993;366:324–7.
38. Seebach D, Beck AK, Bierbaum DJ. The world of beta and gamma-peptides comprised of homologated proteinogenic amino acids and other components. Chem Biodivers. 2004;1:1111–239.
39. Amorin M, Castedo L, Granja JR. Folding control in cyclic peptides through N-methylation pattern selection: formation of antiparallel beta-sheet dimers, double reverse turns and supramolecular helices by 3 alpha,gamma cyclic peptides. Chem Eur J. 2008;14:2100–11.
40. Matsuura K, Murasato K, Kimizuka N. Artificial peptide-nanospheres self-assembled from three-way junctions of beta-sheet-forming peptides. J Am Chem Soc. 2005;127:10148–9.
41. Murota K, Sakamoto S, Kudo K. Orientation control of self-stacking D,L-Alternating cyclic octa-alpha-peptide through multiple electrostatic interactions. Chem Lett. 2007;36:1070–1.
42. Reiriz C, Brea RJ, Arranz R, Carrascosa JL, Garibotti A, Manning B, Valpuesta JM, Eritja R, Castedo L, Granja JR. alpha, gamma-peptide nanotube templating of one-dimensional parallel fullerene arrangements. J Am Chem Soc. 2009;131:11335–7.
43. Ishihara Y, Kimura S. Peptide nanotube composed of cyclic tetra-ss-peptide having polydiacetylene. Biopolymers. 2012;98:155–60.
44. Tabata Y, Uji H, Imai T, Kimura S. Two one-dimensional arrays of naphthyl and anthryl groups along peptide nanotube prepared from cyclic peptide comprising α and β-amino acids. Soft Matter. 2018;14:7597–604.
45. Tabata Y, Mitani S, Kimura S. Peptide nanotube aligning side chains onto one side. J Pept Sci. 2016;22:391–6.
46. Kamano Y, Tabata Y, Uji H, Kimura S. Chiral and random arrangements of flavin chromophores along cyclic peptide nanotubes on gold influencing differently on surface potential and piezoelectricity. RSC Adv. 2019;9:3618–24.
47. Ishihara Y, Kimura S. Four-peptide-nanotube bundle formation by self-assembling of cyclic tetra-beta-peptide using G-quartet motif. Biopolymers. 2013;100:141–7.
48. Tabata Y, Takagaki K, Uji H, Kimura S. Piezoelectric property of buncled peptide nanotubes stapled by bis-cyclic beta-peptide. J Pept Sci. 2018. https://doi.org/10.1002/psc.3134.
49. Ueda M, Uesaka A, Kimura S. Selective disruption of each part of Janus molecular assemblies by lateral diffusion of stimuli-responsive amphiphilic peptides. Chem Commun. 2015;51:1601–4.
50. Hara E, Ueda M, Makino A, Hara I, Ozeki E, Kimura S. Factors influencing in vivo disposition of polymeric micelles on multiple administrations. Acs Med Chem Lett. 2014;5:873–7.

Shunsaku Kimura was born in Kyoto, Japan in 1954. He received his B.S. (1976), M.S. (1978), and Ph.D. (1982, Professor Y. Imanishi) degrees from Kyoto University. He joined the Department of Polymer Chemistry, Kyoto University, as Research Associate (1981), Lecturer (1992), and Associate Professor (1993). He moved to the Department of Material Chemistry, Kyoto University (1996), and in 1999 he was appointed Full Professor. He spent his postdoctoral career (1982−1984, 1986, Professor R. Schwyzer) at ETH-Zurich, Switzerland. He received the Award of the Society of Polymer Science, Japan, in 1999. His main interests are polymer supramolecular chemistry, peptide engineering, theranostic agents, immune-activating or suppressing materials, and optoelectronics nano-devices.